crystals

MDPI

Article

Cyclodextrin-Driven Formation of Double Six-Ring (D6R) Silicate Cage: NMR Spectroscopic Characterization from Solution to Crystals

Mohamed Haouas [1,*], Clément Falaise [1], Charlotte Martineau-Corcos [1,2] and Emmanuel Cadot [1]

1 Institut Lavoisier de Versailles, Centre National de la Recherche Scientifique, Université de Versailles St-Quentin, Université Paris-Saclay, 45 av. des Etats-Unis, 78035 Versailles CEDEX, France; clement.falaise@uvsq.fr (C.F.); charlotte.martineau@uvsq.fr (C.M.-C.); Emmanuel.cadot@uvsq.fr (E.C.)

2 Centre National de la Recherche Scientifique, Conditions Extrêmes et Matériaux: Haute Température et Irradiation, Université d'Orléans, 45071 Orléans, France

* Correspondence: mohamed.haouas@uvsq.fr; Tel.: +33-139-254-254

Received: 21 November 2018; Accepted: 5 December 2018; Published: 7 December 2018

Abstract: Identification and isolation of secondary building units (SBUs) from synthesis media of zeolites still represent a challenging task for chemists. The cage structure anion $Si_{12}O_{30}{}^{12-}$ known as the double six-ring (D6R) was synthesized from α-cyclodextrin (α-CD) mediated alkaline silicate solutions and conditions of its stability and reactivity in aqueous solution were studied by using nuclear magnetic resonance (NMR) spectroscopy. A single crystal X-ray diffraction (XRD) analysis revealed a novel polymorph of the hybrid complex $K_{12}Si_{12}O_{30}{\cdot}2\alpha$-CD$\cdot n D_2O$ ($n \approx 30$–40), which crystallizes in the orthorhombic $C222_1$ space group symmetry with a = 14.841(4) Å, b = 25.855(6) Å, and c = 41.91(1) Å. The supramolecular adduct of the silicate anion sandwiched by two α-CDs forms a perfect symmetry matching the H-bonding donor-acceptor system between the organic macrocycle and the D6R unit. The driving force of such a hybrid assembly has found to be strongly dependent on the nature of the cation present as large alkali counter ions (K^+, Rb^+ and Cs^+), which stabilize the D6R structure acting as templates. Lastly, we provided the first ^{29}Si MAS NMR measurement of ^{3}Q Si in an isolated D6R unit that allows the verification of the linear correlation between the chemical shift and <SiOSi> bond angle for ^{3}Q Si species in D*n*R cages (n = 3, 4, 6).

Keywords: crystallization; nuclear magnetic resonance spectroscopy; hydrogen-bonding; silicate oligomers; self-assembly; molecular recognition; template effect

1. Introduction

Zeolites including both natural and synthetic minerals have been extensively studied over the years because of their structural and chemical properties that produce interest in various fields. Zeolites are associated with ordered micro porosity, high crystallinity, strong acidity, molecular sieving capability or huge specific surface area availability [1], which makes them interesting materials for adsorption [2], catalysis [3,4], and separation [5]. These materials are usually synthesized by the hydrothermal method from hydrolysis-polycondensation of silicates or aluminosilicates in alkaline media [6]. They have several structural characteristics in common based on three-dimensional combinations of TO_4 (T = Si or Al) tetrahedra interconnected to each other by sharing their oxygen atoms. Such molecular arrangements with variable T—O—T bond lengths and angles result in a variety of the so-called Secondary Building Units (SBUs). To date, 23 distinct SBUs are enumerated and proposed by the structure commission of the International Zeolite Association, which allows the structural description of the 235 known zeolitic framework topologies [7]. Some SBU-type silicates

have been identified in solution by using ^{29}Si nuclear magnetic resonance (NMR) spectroscopy [8,9]. Generally, silicates exist as soluble polymeric poly-anions with limited nuclearity, which rarely exceed 10–12 Si atoms, and have a tendency to self-condense as much as possible to favor cycle and cage structures. Nevertheless, structures with large cycles exceeding five Si-based rings have been never detected in synthesis medium. The relationship between soluble silicates and SBUs in solid state is still ambiguous and evidencing 'real' SBUs in solution and their evolution until solid formation currently represents a major scientific challenge [10].

In an early work, Benner et al. reported the isolation and X-ray diffraction (XRD) structure of a potassium dicyclohexasilicate-α-cyclodextrin adduct, $K_{12}Si_{12}O_{30}\cdot 2\alpha$-CD$\cdot 36H_2O$ [11]. It represents a composite molecular assembly including a double six-ring (D6R) silicate anion and two oligosaccharide components involved in a perfect-sandwiched donor-acceptor hydrogen-bond system. The ability of CDs to form inclusion complexes and hybrid adducts with inorganic objects through weak supramolecular interactions including electrostatic forces, H-bonding, chaotropic, and hydrophobic repulsion-attractions is well-documented [12–14]. Their employment as complexing agents may, thus, result in shifting thermodynamic equilibriums and entrapping novel or elusive species because of maximizing entropy by reducing solvation energy. For instance, recently, we demonstrated that introduction of γ-CD modified the speciation in molybdate and tungstate solutions favors the Lindqvist-type poly-anion that has never been observed before in aqueous solution [15]. It, therefore, appears clear that α-CD assists the construction of the D6R unit ($Si_{12}O_{30}{}^{12-}$) and greatly contributes to its stabilization because formation of such a silicate anion is known to not occur spontaneously in aqueous alkaline silicate solutions.

The titled compound $K_{12}Si_{12}O_{30}\cdot 2\alpha$-CD, abbreviated D6R@α-CD hereafter, deserves attention because it represents the unique molecular form known of the hexagonal-prismatic D6R cage while the trigonal-prismatic D3R and the cubic D4R silicate cages are common molecular features occurring in silicate hydrates as tetraalkylammonium salts [16,17]. Furthermore, the D6R unit is the main SBU for CHA, EMT, FAU, GME, and KFI-type zeolites [7]. The host-guest chemistry taking place in D6R@α-CD may help us better understand the complex template effect during the organic-assisted solution and colloidal zeolite crystallization. In this work, we performed a detailed study on the formation of D6R@α-CD in solution by means of ^{1}H and ^{29}Si NMR providing the first NMR spectroscopic characterization of the isolated molecular form of the D6R silicate anion. Moreover, novel crystallographic structure data are reported for D6R@α-CD crystallizing in D_2O with different crystal packing system regarding the previously reported XRD structure determination [11]. Lastly, this work represents a case study of complementary approaches bridging synthesis, NMR characterization, and crystal structure.

2. Materials and Methods

2.1. Chemicals

All reagents were of high purity and were used as obtained from Fisher Scientific France (Illkirch Graffenstaden, France), Sigma-Aldrich Chimie (Lyon, France), TCI Europe (Paris, France), and Fluorochem (Hadfield, UK): NaOH (Acros, 100%), KOH (Alpha-Aesar, 85%), RbOH (Aldrich, 50 wt.% aqueous solution), CsOH (Alpha-Aesar, 80%), tetramethylammonium hydroxide, TMAOH (Alpha-Aesar, 25 wt.% aqueous solution), tetraethylammonium hydroxide, TEAOH (Alpha-Aesar, 35 wt.% aqueous solution), tetrapropylammonium hydroxide, TPAOH (Alpha-Aesar, 40 wt.% aqueous solution), tetrabuthylammonium hydroxide, TBAOH (Alpha-Aesar, 40 wt.% aqueous solution), NaCl (Fluka, 100%), KCl (Sigma, 99%), RbCl (Fluka, 100%), CsCl (Acros, 99%), tetraethylorthosilicate, TEOS (Acros, 98%), α-CD (TCI, 98%), and D_2O (99.90% D, Euro-isotope).

2.2. Synthesis of $K_{12}Si_{12}O_{30}$·2α-CD·36H_2O (D6R@α-CD)

The synthesis of D6R@α-CD is first reported by Benner et al. using tetramethylorthosilicate (TMOS), KOH, and α-CD [11]. In our procedure, TEOS is used as a silicon source. The synthesis was also successfully achieved with silica but the process was much slower. We, therefore, decided to perform all our studies with TEOS.

In typical synthesis, 100 mg (1.78 mmol) of KOH is first dissolved in 1 mL of D_2O to which 250 mg (0.26 mmol) of α-CD is added under magnetic stirring until complete dissolution. Then 320 mg (1.54 mmol) of TEOS is introduced and, to force the hydrolysis, the mixture is vigorously stirred magnetically (1400 rpm) for 15 min. This mixing stage is crucial. It should be long enough to obtain a homogeneous clear phase after complete hydrolysis but also not too long (less than 30 min) because prolonged stirring leads to white insoluble precipitate. The final chemical composition is 1 α-CD:6 SiO_2:6 KOH:24 EtOH:300 D_2O and the pD is 12.7. Crystals with plate shape, suitable for single crystal XRD analysis, are obtained within three days. The addition of KCl up to 30 equivalents accelerates the crystallization and leads to a bigger amount of crystalline product. It is worth noting that, when H_2O is used instead of D_2O, no crystallization happens. It seems that D_2O favors crystallization of D6R@α-CD. Isotopic effect of H_2O/D_2O on crystallization has been observed in some specific systems [18] and is attributed to some physical property changes of the solvent like density or viscosity, which significantly affect the solvation and the diffusivity of solutes [19].

The product was characterized by single crystal XRD, FT-IR spectroscopy, thermogravimetric analysis (TGA), solid-state ^{13}C and ^{29}Si magic-angle spinning (MAS) NMR, and, in solution, by ^{1}H and ^{29}Si NMR spectroscopy (50 mg in 0.5 mL D_2O). XRD and NMR results will be discussed in Section 3. FT-IR spectrum and TGA curve are shown in Supplementary Materials (Figures S1 and S2). IR shows the characteristic bands for α-CD at 1648, 1432, 1360, 1156, and 1000 cm^{-1} and others are assigned to silicate groups at 1108, 1184, 1000, and 464 cm^{-1}. Other important absorption bands are visible at 3344, 2926, and 667 cm^{-1}. TGA reveals a weight loss of about 17% from 25 °C to 240 °C (the expected weight loss for 36 H_2O is 16.70%).

2.3. Nuclear Magnetic Resonance (NMR) Study in Solution

Synthesis solutions with variable chemical composition were studied by ^{1}H and ^{29}Si NMR spectroscopy to establish optimal experimental conditions for the formation of the composite complex D6R@α-CD. The following systems have been prepared according to the same procedure of Section 2.2 to study:

(i) kinetics: 1 α-CD:6 TEOS:6 KOH:300 D_2O
(ii) effect of KCl: 1 α-CD:6 TEOS:6 KOH:y D_2O:x KCl (y = 600–1000, x = 15–60)
(iii) effect of base: 1 α-CD:6 TEOS:6 XOH:200 D_2O (X = Na, K, Rb, Cs, TMA, TEA, TPA, TBA)
(iv) effect of cation: 1 α-CD:6 TEAOH:900 D_2O:40 XCl (X = Na, K, Rb, Cs)

2.4. Characterization Techniques

2.4.1. NMR Spectroscopy

Liquid state spectra were measured in D_2O at 24 °C using standard Quartz 5 mm NMR tubes. A fixed amount of 0.5 mL for each sample was analyzed on a Bruker Avance 400 spectrometer (Karlsruhe, Baden-Württemberg, Germany) operating at a Larmor frequency of 400.1 and 79.49 MHz for ^{1}H and ^{29}Si, respectively. The ^{29}Si spectra were acquired with a Hahn-echo sequence to minimize the probe background signal as much as possible. Typically, spectra at a spectral width of 6.25 kHz and a digital resolution of 0.4 Hz per point were measured with 16384 scans and a repetition rate of 4 s/scan.

Solid state $^{13}C\{^{1}H\}$ and $^{29}Si\{^{1}H\}$ NMR spectra were recorded with a Bruker Avance 500 spectrometer (Karlsruhe, Baden-Württemberg, Germany) equipped with a 4 mm H/X MAS probe,

operating at a Larmor frequency of 500.1, 125.8, and 99.35 MHz for ^{1}H, ^{13}C, and ^{29}Si, respectively. Samples were filled into a 4 mm ZrO_2 rotor and spun at 10 kHz for direct polarization (DP) or cross polarization (CP) experiments under high-power ^{1}H decoupling. No significant difference in relative signal intensities between spectra recorded with DP or CP conditions indicates quantitative measurements. ^{29}Si CPMAS NMR spectra were recorded with a 5 s recycle delay and 750 transients.

All experimental data were zero-filled to double the number of experimental points. Chemical shifts were calibrated with respect to standard tetramethylsilane, TMS (0.0 ppm), for all nuclei, i.e., ^{1}H, ^{13}C, and ^{29}Si. Spectral decomposition was performed by using NMRNoteBook software (NMRTEC, Illkirch Graffenstaden, France).

2.4.2. Fourier Transform Infrared (FT-IR) and Thermogravimetric Analysis (TGA)

FT-IR spectra were recorded on a 6700 FT-IR Nicolet spectrophotometer (Madison, WI, USA) using the diamond ATR technique. The spectra were recorded on non-diluted compounds at a solid state in the 400–4000 cm^{-1} range using ATR correction. TGA curves were obtained by using a Mettler Toledo TGA/DSC 1, STAR^{e} System instrument (Giessen, Hesse, Germany). The temperature was measured with an accuracy of ± 1 K. The analysis was carried out in an air flow at a heating rate of 5 K/min^{-1}. About 10 mg of the powder sample was used.

2.4.3. Single Crystal X-ray Diffraction (XRD)

Crystallographic data for single-crystal X-ray diffraction study are summarized in Table 1. These data can be obtained free of charge from The Cambridge Crystallographic Data Center via https://www.ccdc.cam.ac.uk/structures-beta/under deposit number: 1879607.

Table 1. Crystal data and structure refinement parameters for D6R@α-CD.

Empirical Formula	**$K_{12}Si_{12}C_{72}H_{192}O_{126}$ ($K_{12}Si_{12}O_{30}$·2α-CD·36H_2O)**
Formula weight	3880.44
Temperature/K	230(2)
Crystal system	Orthorhombic
Space group	$C222_1$
a/Å	14.841(4)
b/Å	21.855(6)
c/Å	41.91(1)
α/°	90
β/°	90
γ/°	90
Volume/Å^3	16,081(7)
Z	4
ρ_{calc}/gcm^{-3}	1.603
μ/mm^{-1}	0.515
F(000)	7104
Crystal size/mm^3	0.2 × 0.13 × 0.08
Radiation	Mo Kα (λ = 0.71073)
2Θ range for data collection/°	5.0 to 50.1
Index ranges	$-17 \leq h \leq 17$, $-30 \leq k \leq 30$, $-49 \leq l \leq 49$
Reflections collected	69910
Independent reflections	14,190, $R_{int} = 0.0697$, $R_{sigma} = 0.0523$
Data/restraints/parameters	14,190/6/891
Goodness of fit on F^2	1.048
Final R indexes [I > = 2σ (I)]	$R_1 = 0.0778$, $wR_2 = 0.2185$
Final R indexes [all data]	$R_1 = 0.0844$, $wR_2 = 0.2245$
Largest diff. peak/hole/eÅ^{-3}	1.69/−1.54
Flack parameter	0.13(9)

Crystals of D6R@α-CD were selected under a polarizing optical microscope and glued in paratone oil to prevent any loss of crystallization water. X-ray intensity data were collected at a low temperature (T = 230 K) on a Bruker D8 VENTURE diffractometer (Karlsruhe, Germany) equipped with a

PHOTON 100 CMOS bidimensional detector using a high brilliance IμS micro-focus X-ray Mo Kα mono-chromatized radiation (λ = 0.71073 Å). Data reduction was accomplished by using SAINT V7.53a. The substantial redundancy in data allowed a semi-empirical absorption correction (SADABS V2.10) to be applied based on multiple measurements of equivalent reflections. Using Olex2 [20], the structure was solved with the ShelXT structure solution program [21] using Intrinsic Phasing, and refined with the ShelXL [22] refinement package using Least Squares minimization. Numerous water molecules located inside the cavities were disordered. Thereby, the contribution of solvent-electron density was removed using the SQUEEZE routine in PLATON [23], which produced a set of solvent-free diffraction intensities. The remaining non-hydrogen atoms were located from Fourier differences and were refined with anisotropic thermal parameters. Positions of the hydrogen atoms belonging to the α-CD were calculated and refined isotropically by using the gliding mode.

3. Results and Discussions

3.1. XRD Structure and NMR Characterization of D6R@α-CD

The supramolecular adduct D6R@α-CD crystallizes in the orthorhombic space group $C222_1$ with cell parameters: a = 14.841(4) Å, b = 25.855(6) Å, and c = 41.91(1) Å, V = 16081(7) $Å^3$. The crystallographic data of the literature are different with a space group P1 (triclinic) and cell parameters a = 14.779(2) Å, b = 21.620(3) Å, c = 25.680(4) Å, α = 98.41(1)°, β = 91°, γ = 107.28(1)°, V = 7734.1 $Å^3$ [11], which means we present a different polymorph. The structure analysis revealed a sandwich complex comprising the prismatic dicyclohexasilicate anion $[Si_{12}O_{30}]^{12-}$ (D6R) intercalated between two α-CD molecules. Such assembly shown in Figure 1a,b also contains two potassium cations centered on the top and bottom bases of the hexagonal cage. Each potassium atom shows six direct contacts to bridging oxygen in the hexagonal window with d(K—O) = 2.8–3.0 Å. These potassium cations may play an important structural role to aid in maintaining the hybrid assembly. The crystal packing is very similar to the published triclinic form with an identical basic motif of the inorganic-organic assembly stacked in a way to form silicate layers alternating with organic cyclodextrin double layers along hexagonal rods (Figure S3 in Supplementary Materials). However, the disposition of the remaining 10 potassium atoms surrounding the D6R unit is different in the two polymorphic forms. Considering the silicate cage and their 12 potassium counter ions, no symmetry is present in the triclinic form (Figure S4 in Supplementary Materials) while the orthorhombic form presents a C_2 symmetry axis (Figure 1c,d). This difference between the two crystallographic systems appears due to the positions of the potassium atoms around the cyclodextrin-silicate assembly.

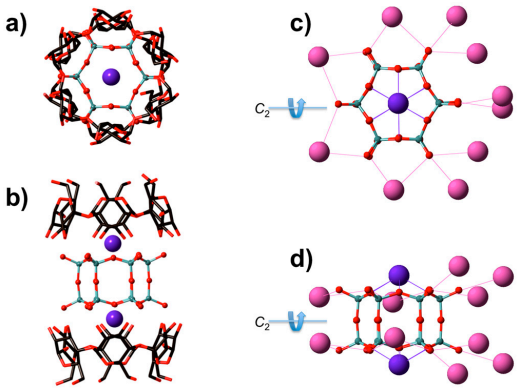

Figure 1. Crystallographic top (**a**,**c**) and side (**b**,**d**) views of D6R@α-CD with respect to the D_6 symmetry axis of the prismatic silicate cage. In (**a**,**b**), the environment of the α-CD in the adduct is highlighted while, in (**c**,**d**), the location of the 10 peripheral potassium around the D6R is shown. The two potassium atoms positioned on the top and bottom sides of the prismatic cage are shown in both cases with a different color code. Grey: Si, Red: O, and Blue/Purple: K. Hydrogen are not shown for the sake of clarity.

The distances between the peripheral K^+ and the terminal deprotonated silanols (Si—O^-) are within the range of 3.3–3.9 Å, which indicates there is no direct contact between these potassium and the silicate anions. Thus, they should be involved in a common H-bonding network through water molecules. Because our structure is obtained in D_2O, we may infer that the isotopic effect of heavy water has enforced a different H/D-bonding structure around the potassium cations, which, in turn, has led to different polymorphic structure. Consequently, the local symmetry of the hybrid assembly is higher in the orthorhombic form than the triclinic structure.

The driving force for the formation of the supramolecular adduct D6R@α-CD would be the mutual interaction between the silicate cage and the α-CD molecules forming a strong donor-acceptor H-bonding network. The 12 hydroxyl groups of each CD at the secondary rim are involved in H-bond contacts with the six terminal deprotonated silanol groups of each hexagonal face, which exhibits interatomic O—O distances within the range 2.5–2.8 Å.

In the original paper by Benner et al. [11], no spectroscopic data of D6R@αCD were provided. We report in this paper the first ^1H and ^{29}Si NMR characterization of the silicate-CD complex in D_2O (Figure 2). The adduct was not stable in pure D_2O but dissolution of the crystalline product in alkaline solution (pD = 12.7) and rich in potassium (3 M KCl) allows its stabilization.

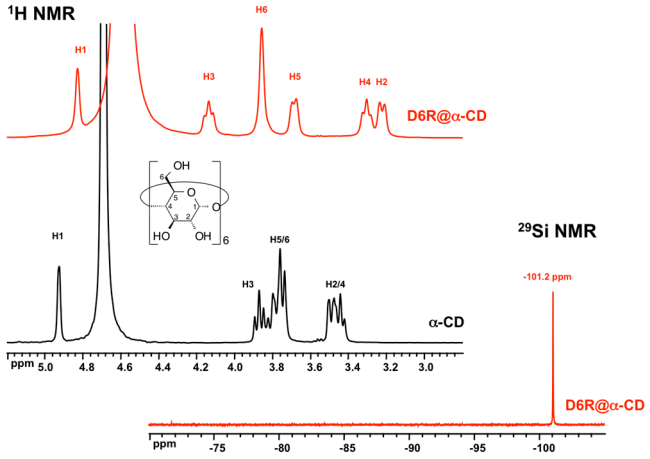

Figure 2. ^1H and ^{29}Si NMR spectra of D6R@α-CD (15 mM in 3 M KCl D_2O, pD = 12.7). For comparison, the spectrum of a solution of α-CD (30 mM in D_2O) is also shown.

The ^1H NMR exhibits the six types of protons of the CD labeled H1 to H6, which underwent substantial changes of their position in D6R@αCD when compared to the original spectrum of αCD. However, the difference in chemical shifts differed from a proton type to another, as illustrated in Table 2. These effects represent a specific signature of involvement of the CD tori in the mutual donor-acceptor interaction within the adduct. The hydrogen bonding system, which fixes the conformation of the toroidal oligosaccharide, would affect the environment of the protons at different extent depending on their position in the molecule with respect to the interacting rim. The most important changes in chemical shifts are observed for protons H2 and H3, which are present on the interacting side with the silicate anion, while the least effects are observed for protons H5 and H6 located at the opposite side. The ^{29}Si NMR spectrum exhibits a single signal at −101.2 ppm corresponding to the 12 equivalent Si in the D6R unit. This result highlights the high symmetry of the adduct in an idealized D_6 environment. The observed chemical shift appeared at the high-field limit of typical chemical shifts range for the Q^3 $OSi(OSi)_3$ environment (from −94 to −101 ppm) [24] and represents the first known example of the D6R anion in aqueous solution. This chemical shift also compares well with the values for the cubic octamer D4R observed to range from −98.1 to −100.0 ppm [8,9,25].

Table 2. Comparison of ^{1}H NMR chemical shifts [1] of D6R@α-CD with respect to the free α-CD.

	H1	H2	H3	H4	H5	H6
α-CD	4.92	3.49	3.87	3.44	3.75	3.78
D6R-α-CD	4.83	3.22	4.14	3.30	3.69	3.86
Δδ(ppm)	+0.09	+0.27	−0.27	+0.14	+0.06	−0.08

[1] Accuracy = ± 0.01 ppm.

3.2. Formation and Stability of D6R@α-CD in Solution

The synthesis of D6R@α-CD takes place in a concentrated solution containing stoichiometric amounts of α-CD, TEOS, and KOH. To investigate the synthesis medium, ^{1}H and ^{29}Si NMR were recorded immediately after the complete hydrolysis of TEOS in the system 1 α-CD:6 TEOS:6 KOH:300 D_2O. The expected NMR signatures of the adduct D6R@α-CD observed in Figure 2 were not present. We, therefore, monitored the kinetics of formation by recording NMR measurements over a long period up to nine days of aging. These measurements shown in Figures 3 and 4 revealed a very slow formation process where the adduct reached a maximum yield of ca. 45% after five days. The NMR signature of D6R in Figure 4 coincides with the appearance of the specific ^{1}H NMR signals of complexed CD in Figure 3, which means that they should exist only as a composite D6R-CD adduct. ^{29}Si NMR can monitor the slow formation of the D6R silicate, which is shown in Figure 4. The signals of monomers at −72 ppm and other oligomers visible between −80 and −100 ppm decreased progressively as a function of time while the resonance of the D6R appearing at −101 ppm increased continuously to reach 41% of total Si signals after five days of aging. These observations are consistent with the ^{1}H NMR results of Figure 3 and demonstrate the slow conversion of small silicate oligomers into the D6R unit. In order to improve the D6R-αCD production, we studied the effect of the addition of KCl in the synthesis medium (Figure S5 in Supplementary Materials). The addition of potassium salt allows the enrichment of the medium in potassium without altering the pD, which is a crucial parameter for the synthesis. The yield, as expected, increased significantly by introducing KCl, but to a certain limit due to the KCl solubility. To introduce more KCl, we had to dilute the system further, which also affects the synthesis by lowering the yield. A compromise between dilution and KCl addition has to be found for optimal yield and the highest value obtained was 68% for the system 1 α-CD:6 TEOS:6 KOH:700 D_2O:30 KCl.

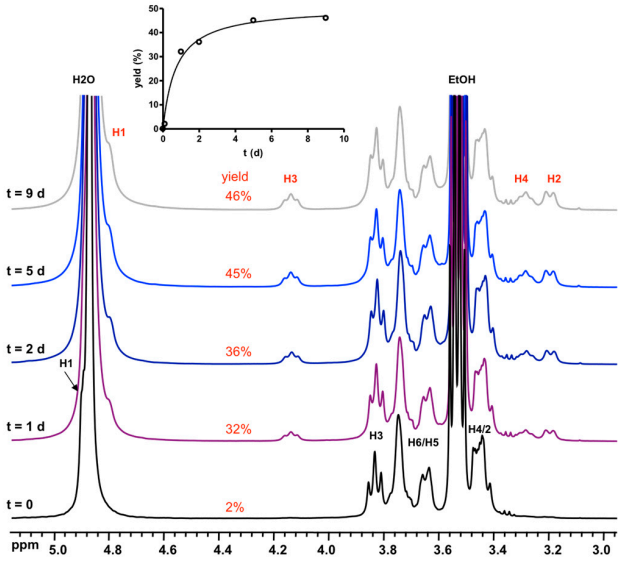

Figure 3. Evolution of ^{1}H NMR spectra of the synthesis medium in the system 1 α-CD:6 TEOS:6 KOH:300 D_2O with time, showing the growth of signals of D6R@α-CD. Inset: plot of the progressive increase of the yield with time measured from the signal of H3 at ca. 4.1 ppm.

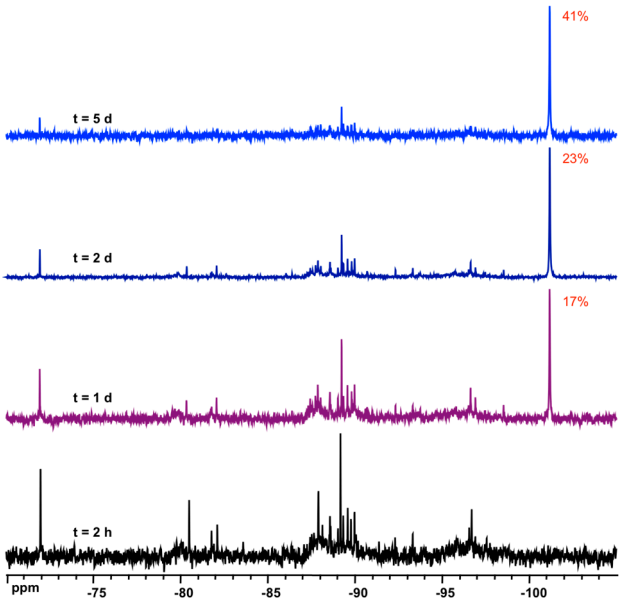

Figure 4. Evolution of ^{29}Si NMR spectra of the synthesis medium in the system 1 α-CD:6 TEOS:6 KOH:300 D_2O with time, which shows the growth of the signal of D6R@α-CD at ca. 101 ppm.

To investigate the effect of the base, several mineral and organic bases were studied in the system 1 α-CD:6 TEOS:6 base:300 D_2O. When LiOH or NH_4OH is used, white precipitates were formed presumably as amorphous silicates. In the case of NaOH, two distinct separate liquid phases were obtained. De-mixing into two non-miscible phases and formation of hydrated silicate ionic liquid (HSIL) are known to occur in such a highly alkaline mineral system [26]. Such a phenomenon did not, however, happen with KOH, RbOH, or CsOH and a clear homogeneous phase was observed, which indicates that the presence of α-CD modified the chemistry of these solutions in contrast to the system containing NaOH. Figure 5 shows the ^{29}Si NMR spectra of the equilibrated solutions using NaOH, KOH, RbOH, CsOH, TMAOH, TEAOH, TPAOH, or TBAOH as a base for TEOS hydrolysis in the presence of α-CD. The characteristic signal at ca. −101 ppm indicates that the presence of D6R is observed only in systems containing large alkali cations, i.e., K^+, Rb^+, and Cs^+. In the case of Na^+ and TAA^+ cations, no D6R units can be observed and only the usual silicate oligomers were present with these cations especially D4R and D3R units in TMA and TEA solutions [25,27,28].

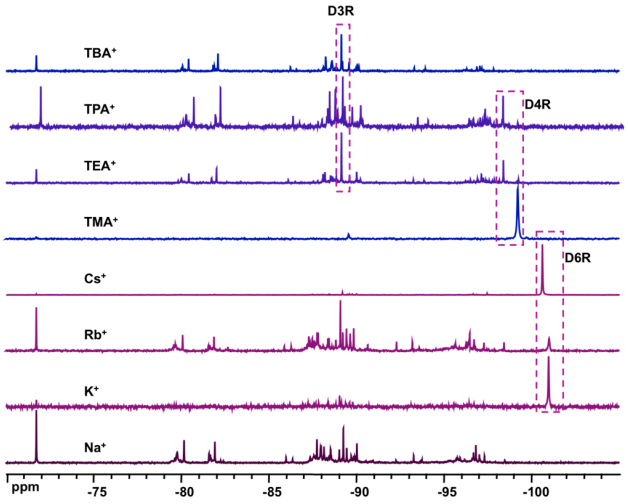

Figure 5. ^{29}Si NMR spectra of equilibrated solutions in the system 1 α-CD:6 TEOS:6 base:300 D_2O, base = NaOH, KOH, RbOH, CSOH, TMAOH, TEAOH, TPAOH, and TBAOH, which shows the occurrence of D6R (ca. 101 ppm) with the presence of large alkali cations (K^+, Rb^+, and Cs^+).

To further study the effect of alkali cation on the formation of D6R@α-CD, chloride salts of sodium, potassium, rubidium, or cesium were introduced to a silicate solution containing α-CD in the system 1 α-CD:6 TEOS:6 TEAOH:900 D_2O. The adduct D6R@α-CD was not favored in tetraalkylammonium silicate solutions and the introduction of alkali cations in large excess had led to the adduct formation only in the case of K^+, Rb^+, and Cs^+ with 67%, 55%, and 90% yield, respectively (Figure 6). With Na, however, no such complex occurred. These results are fully consistent with the previous study of alkali bases confirming that D6R@α-CD is stabilized by K^+ and Cs^+ and, to a lesser extent, Rb^+. This, however, contrasts with the original paper of Benner et al. [11] who stated that potassium ions do not have a significant influence on the formation of D6R@α-CD since a similar complex has also been obtained with sodium cations. According to our results, it appears that the alkali cation size plays a crucial role to stabilize the D6R cage by binding to the coordinating sites of the prism bases. The cesium cation offers an optimal size while the sodium ion is unfavorably small to template the six-ring window.

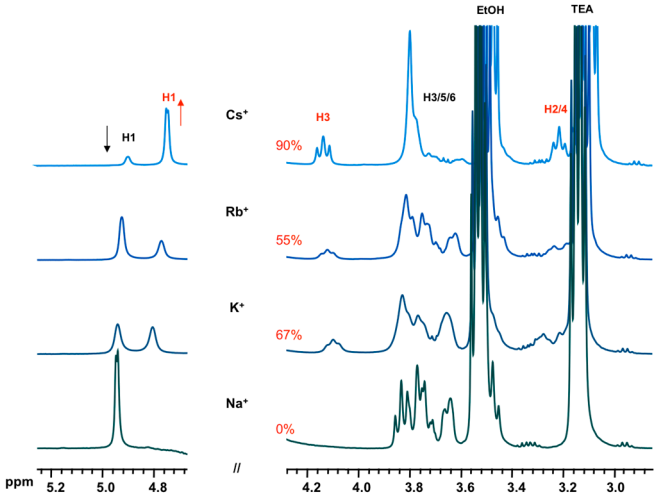

Figure 6. ^1H NMR spectra of equilibrated solutions in the system 1 α-CD:6 TEOS:6 TEAOH:900 D_2O:40 XCl, X = Na, K, Rb, and Cs, which shows the dependence of D6R@α-CD (ca. 4.1 ppm) on the nature of the alkali cation.

Attempts were undertaken to poly-condensate the obtained D6R units from their native solution by hydrothermal treatment to produce porous materials from prefabricated SBU. Unfortunately, no tridimensional porous materials were obtained but, instead, crystalline layered potassium hydrogen disilicate $KHSi_2O_5$ polymorphs [29,30] were formed, which were also obtained in the same system without α-CD. To investigate the effect of the temperature on the stability of the D6R@α-CD unit, NMR experiments were conducted at 55 °C (see Figures S6 and S7 in Supplementary Materials). These experiments revealed the instability of the D6R@α-CD adduct upon heating as the characteristic ^1H and ^{29}Si NMR signals completely disappeared at 55 °C. By lowering the temperature to room condition, the D6R@α-CD adduct reappeared again slowly. These results suggest the composite complex D6R@α-CD is fragile and decomposes easily by heating even though the assembly-disassembly process is reversible with the temperature.

3.3. Solid State NMR Characterization

The D6R@α-CD compound was analyzed by means of ^{13}C and ^{29}Si solid state NMR spectroscopy. The ^{13}C CPMMAS spectrum (see Figure S8 in Supplementary Materials) exhibits the characteristic signals of the six carbon types of α-CD in the organic moiety and the spectrum compares well with that of the parent α-CD. Some resolutions can be seen for each site as an indication of several local environments around each glucopyranose groups. Figure 7 shows the ^{29}Si MAS NMR spectrum of D6R@α-CD revealing signals in the range −101 to −103 ppm. Spectral decomposition allows the

distinction of four resonances with a signal area ratio of 1:3:1:1. Such a distribution could account for the non-resolved six Si types (2 Si:3 × 2 Si:2 Si:2 Si) in the D6R@α-CD adduct by taking into account the potassium environments. The local potassium silicate ensemble exhibits a C_2 symmetry (see Figure 1c,d) leading to six inequivalent pairs of Si in the D6R unit. The observed chemical shifts compare well with the value measured in aqueous solution, i.e., −101 ppm (Figure 2), but fall at a slightly higher field outside the typical range for Q^3 type Si in silicates [31]. Distortion of the bond angles in the silicon-oxygen tetrahedra and variations in SiOSi bond angles could cause significant changes of ^{29}Si shifts. A linear relationship between ^{29}Si chemical shifts and SiOSi angles of silicates is well-established for Q^4 type Si sites as expressed in equation 1 [32].

$$\delta(\text{ppm}) = -0.6192 \text{ <SiOSi> } -18.68, \text{ R} = 0.974 \quad (1)$$

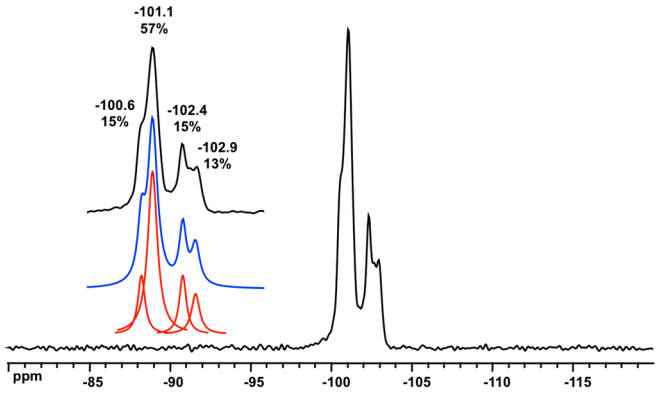

Figure 7. ^{29}Si MAS NMR spectrum of D6R@α-CD. Inset: spectral decomposition showing four sites in a 1:3:1:1 ratio.

Table 3 summarizes the mean SiOSi angle observed in D6R@α-CD and in other silicate cage structures such as D3R and D4R for comparison. In strained D3R structure, the mean SiOSi angle is the smallest in the 3R face. However, the mean SiOSi angle in the 6R face of D6R@α-CD is not larger than the mean SiOSi angle in the cubic D4R compound, which means that there are no particular structural constraints in these structures. Nevertheless, the mean SiOSi angle in the 4R face increases significantly with an increasing n in DnR from ca. 130 to 150 to 170° for n = 3, 4, or 6. This means the prismatic shape of these cages becomes more elongated in the series from D3R to D6R. Because of these structural features, the average SiOSi bond in these Q^3 Si increases progressively from D3R to D6R, which would explain the linear variation in ^{29}Si chemical shifts shown in Figure 8. A relationship between observed Q^3 ^{29}Si shifts in the DnR and mean SiOSi angle is derived (equation 2), which is similar to that for Q^4 sites in silicates. The two linear relations have almost the same slope (ca. −0.6 ppm/°) and a difference of Y-intercept of ca. 7 ppm, which corresponds to the well-established condensation effect between Q^4 and Q^3. This means this relationship could be generalized for Q^n sites considering the difference in the Y-intercept as due to a Q^n condensation effect.

$$\delta(\text{ppm}) = -0.5824 \text{ <SiOSi> } -11.51, \text{ R} = 0.982 \quad (2)$$

Table 3. Mean SiOSi bond angles in D*n*R silicate compounds and ^{29}Si NMR data.

Environment	Mean SiOSi (°)	Average SiOSi (°)	^{29}Si (ppm)	References
D3R/3R [1]	131.0 (×6) [2]	134.3	−89.6	[16]
D3R/4R	141.3 (×3)			[16]
D4R/4R	from 147.9 to 150.5		−98.4 to −100.2	[17,33–35]
D6R/6R	144.8 (×12)	154.3	−101.2 to −101.5	this work
D6R/4R	173.3 (×6)			this work

[1] *n*R to the *n*-ring faces of the oligo-anion in which the bridging O atoms are involved. [2] Multiplicity.

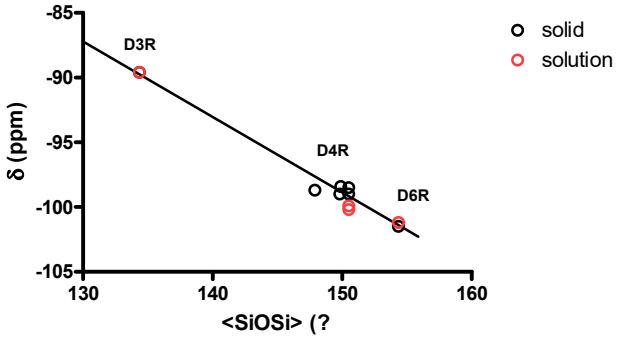

Figure 8. Relation between ^{29}Si chemical shift and mean SiOSi angle for Q^3 Si in silicate cages D*n*R.

4. Conclusions

The D6R silicate poly-anion is prepared in alkaline media in the presence of α-CD that stabilizes the cage structure through an elaborated acceptor-donor H-bonding network, which leads to a sandwich supramolecular adduct. We report in this scenario a novel polymorphic crystallographic form of the hybrid compound D6R@α-CD. Studies in solution revealed the important structural role of potassium cations stabilizing the prismatic structure with large 6R faces. Such a template effect is also observed with bulkier alkali cations namely Rb^+ and Cs^+. Organic TAA cations, however, did not show such a stabilizing effect. The formation process of the inclusion complex was found to occur slowly at room temperature. Heating is not a favorable factor for the formation of such fragile assembly. The complex was characterized by NMR spectroscopy in solution and solid state. Both ^{1}H and ^{29}Si NMR exhibited characteristic features of complexed α-CD and silicate cage structure. Attempts to rationalize the observed ^{29}Si NMR shifts were made in relation with SiOSi bond angle effects.

Supplementary Materials: The following are available online at http://www.mdpi.com/2073-4352/8/12/457/s1, Figures S1 and S2: FT-IR spectrum and TGA curve of $K_{12}Si_{12}O_{30}$·2α-CD·36H_2O. Figures S3 and S4: Crystallographic structure of $K_{12}Si_{12}O_{30}$·2α-CD·36H_2O. Figure S5: Effect of KCl on ^{1}H NMR of synthesis medium of D6R@α-CD. Figures S6 and S7: Effect of temperature on D6R@α-CD stability. Figure S8: ^{13}C CPMAS NMR of D6R@α-CD.

Author Contributions: Conceptualization, M.H. and E.C. crystallography, C.F. solid state NMR C.M.-C. Methodology, investigation, and data analysis, M.H. Writing—original draft preparation, M.H. Review and editing, C.F., C.M.-C., and E.C.

Funding: This research received no external funding.

Acknowledgments: The authors gratefully acknowledge financial support from the labEx CHARMMMAT of University Paris-Saclay (grant number ANR-11-LABX-0039). CMC thanks the Institut Universitaire de France (IUF) for financial support.

Conflicts of Interest: The authors declare no conflict of interest.

References

1. Li, Y.; Li, L.; Yu, J.H. Applications of Zeolites in Sustainable Chemistry. *Chem* **2017**, *3*, 928–949. [CrossRef]
2. Zecchina, A.; Bordiga, S.; Vitillo, J.G.; Ricchiardi, G.; Lamberti, C.; Spoto, G.; Bjorgen, M.; Lillerud, K.P. Liquid hydrogen in protonic chabazite. *J. Am. Chem. Soc.* **2005**, *127*, 6361–6366. [CrossRef] [PubMed]

3. Chassaing, S.; Beneteau, V.; Pale, P. Green catalysts based on zeolites for heterocycle synthesis. *Curr. Opin. Green Sustain. Chem.* **2018**, *10*, 35–39. [CrossRef]
4. Ennaert, T.; Van Aelst, J.; Dijkmans, J.; De Clercq, R.; Schutyser, W.; Dusselier, M.; Verboekend, D.; Sels, B.F. Potential and challenges of zeolite chemistry in the catalytic conversion of biomass. *Chem. Soc. Rev.* **2016**, *45*, 584–611. [CrossRef] [PubMed]
5. Rangnekar, N.; Mittal, N.; Elyassi, B.; Caro, J.; Tsapatsis, M. Zeolite membranes—A review and comparison with MOFs. *Chem. Soc. Rev.* **2015**, *44*, 7128–7154. [CrossRef] [PubMed]
6. Barrer, R.M. Zeolites and their synthesis. *Zeolites* **1981**, *1*, 130–140. [CrossRef]
7. Database of Zeolite Structures. Available online: http://www.iza-structure.org/databases/ (accessed on 6 December 2018).
8. Haouas, M.; Taulelle, F. Revisiting the identification of structural units in aqueous silicate solutions by two-dimensional silicon-29 INADEQUATE. *J. Phys. Chem. B* **2006**, *110*, 3007–3014. [CrossRef]
9. Knight, C.T.G.; Balec, R.J.; Kinrade, S.D. The structure of silicate anions in aqueous alkaline solutions. *Angew. Chem.-Int. Edit.* **2007**, *46*, 8148–8152. [CrossRef]
10. Haouas, M. Nuclear Magnetic Resonance Spectroscopy for In Situ Monitoring of Porous Materials Formation under Hydrothermal Conditions. *Materials* **2018**, *11*, 1416. [CrossRef]
11. Benner, K.; Klufers, P.; Schuhmacher, J. A molecular composite constructed in aqueous alkaline solution from a double six-ring silicate and alpha-cyclodextrin. *Angew. Chem.-Int. Edit.* **1997**, *36*, 743–745. [CrossRef]
12. Assaf, K.I.; Ural, M.S.; Pan, F.F.; Georgiev, T.; Simova, S.; Rissanen, K.; Gabel, D.; Nau, W.M. Water Structure Recovery in Chaotropic Anion Recognition: High-Affinity Binding of Dodecaborate Clusters to -Cyclodextrin. *Angew. Chem.-Int. Edit.* **2015**, *54*, 6852–6856. [CrossRef] [PubMed]
13. Moussawi, M.A.; Haouas, M.; Floquet, S.; Shepard, W.E.; Abramov, P.A.; Sokolov, M.N.; Fedin, V.P.; Cordier, S.; Ponchel, A.; Monflier, E.; et al. Nonconventional Three-Component Hierarchical Host-Guest Assembly Based on Mo-Blue Ring-Shaped Giant Anion, gamma-Cyclodextrin, and Dawson-type Polyoxometalate. *J. Am. Chem. Soc.* **2017**, *139*, 14376–14379. [CrossRef] [PubMed]
14. Prochowicz, D.; Kornowicz, A.; Lewinski, J. Interactions of Native Cyclodextrins with Metal Ions and Inorganic Nanoparticles: Fertile Landscape for Chemistry and Materials Science. *Chem. Rev.* **2017**, *117*, 13461–13501. [CrossRef] [PubMed]
15. Falaise, C.; Moussawi, M.A.; Floquet, S.; Abramov, P.A.; Sokolov, M.N.; Haouas, M.; Cadot, E. Probing Dynamic Library of Metal-Oxo Building Blocks with gamma-Cyclodextrin. *J. Am. Chem. Soc.* **2018**, *140*, 11198–11201. [CrossRef] [PubMed]
16. Wiebcke, M.; Felsche, J. The tetraethylammonium cation in a double three-ring silicate heteronetwork clathrate and a polyhedral clathrate hydrate: Low-temperature single-crystal X-ray diffraction studies on (NEt4)6Si6O15, 40.8H2O and NEt4OH,9H2O. *Microporous Mesoporous Mater.* **2001**, *43*, 289–297. [CrossRef]
17. Wiebcke, M.; Grube, M.; Koller, H.; Engelhardt, G.; Felsche, J. Structural Links Between Zeolite-Type and Clathrate Hydrate-Type Materials—Redetermination of the Crystal-Structure of (N(CH3)4)8Si8O20.65H2O by Single-Crystal X-Ray-Diffraction and Variable-Temperature MAS NMR-Spectroscopy. *Microporous Mater.* **1993**, *2*, 55–63. [CrossRef]
18. Enkelmann, D.D.; Hofmann, D.W.M.; Merz, K. Deuterium Shifts the Equilibrium: How Heavy Water Can Influence Organic Multicomponent Crystal Formation. *Cryst. Growth Des.* **2017**, *17*, 4726–4729. [CrossRef]
19. Sasmal, D.K.; Dey, S.; Das, D.K.; Bhattacharyya, K. Deuterium isotope effect on femtosecond solvation dynamics in methyl beta-cyclodextrins. *J. Chem. Phys.* **2009**, *131*, 44509. [CrossRef] [PubMed]
20. Dolomanov, O.V.; Bourhis, L.J.; Gildea, R.J.; Howard, J.A.K.; Puschmann, H. OLEX2: A complete structure solution, refinement and analysis program. *J. Appl. Crystallogr.* **2009**, *42*, 339–341. [CrossRef]
21. Sheldrick, G.M. SHELXT—Integrated space-group and crystal-structure determination. *Acta Crystallogr. Sect. A* **2015**, *71*, 3–8. [CrossRef]
22. Sheldrick, G.M. Crystal structure refinement with SHELXL. *Acta Crystallogr. Sect. C-Struct. Chem.* **2015**, *71*, 3–8. [CrossRef]
23. Spek, A.L. PLATON SQUEEZE: A tool for the calculation of the disordered solvent contribution to the calculated structure factors. *Acta Crystallogr. Sect. C-Struct. Chem.* **2015**, *71*, 9–18. [CrossRef]
24. Engelhardt, G.; Michel, D. *High-Resolution Solid-State NMR of Silicates and Zeolites*; John Wiley & Sons: New York, NY, USA, 1987; pp. 75–105.

25. Falcone, J.S.; Bass, J.L.; Krumrine, P.H.; Brensinger, K.; Schenk, E.R. Characterizing the Infrared Bands of Aqueous Soluble Silicates. *J. Phys. Chem. A* **2010**, *114*, 2438–2446. [CrossRef]
26. van Tendeloo, L.; Haouas, M.; Martens, J.A.; Kirschhock, C.E.A.; Breynaert, E.; Taulelle, F. Zeolite synthesis in hydrated silicate ionic liquids. *Faraday Discuss.* **2015**, *179*, 437–449. [CrossRef]
27. Hoebbel, D.; Garzo, G.; Engelhardt, G.; Ebert, R.; Lippmaa, E.; Alla, M. On the Constitution of Silicate Anions in Tetraethylammonium Silicates and their Aqueous Solutions. *Z. Anorg. Allg. Chem.* **1980**, *465*, 15–33. [CrossRef]
28. Caratzoulas, S.; Vlachos, D.G.; Tsapatsis, M. On the role of tetramethylammonium cation and effects of solvent dynamics on the stability of the cage-like silicates Si6O156- and Si8O208- in aqueous solution. A molecular dynamics study. *J. Am. Chem. Soc.* **2006**, *128*, 596–606. [CrossRef]
29. Lebihan, M.T.; Kalt, A.; Wey, R. Structural study of KHSi2O5 and H2Si2O5. *Bull. Soc. Fr. Mineral. Cristallogr.* **1971**, *94*, 15.
30. Schmidmair, D.; Kahlenberg, V.; Perfler, L.; Tobbens, D.M. Structural, spectroscopic and computational studies on the monoclinic polymorph (form I) of potassium hydrogen disilicate (KHSi2O5). *Mineral. Mag.* **2014**, *78*, 609–622. [CrossRef]
31. Magi, M.; Lippmaa, E.; Samoson, A.; Engelhardt, G.; Grimmer, A.R. Solid-state high-resolution Si-29 chemical shifts in silicates. *J. Phys. Chem.* **1984**, *88*, 1518–1522. [CrossRef]
32. Engelhardt, G.; Radeglia, R. A semi-empirical quantum-chemical rationalization of the correlation between SiOSi angles and Si-29 NMR chemical shifts of silica polymorphs and framework aluminosilicates (Zeolites). *Chem. Phys. Lett.* **1984**, *108*, 271–274. [CrossRef]
33. Verlooy, P.L.H.; Robeyns, K.; Van Meervelt, L.; Lebedev, O.I.; Van Tendeloo, G.; Martens, J.A.; Kirschhock, C.E.A. Synthesis and characterization of the new cyclosilicate hydrate (hexamethyleneimine)(4)center dot Si8O16(OH)(4) center dot 12H(2)O. *Microporous Mesoporous Mater.* **2010**, *130*, 14–20. [CrossRef]
34. Wiebcke, M.; Emmer, J.; Felsche, J.; Hoebbel, D.; Engelhardt, G. TMPA4Si8O20.34H2O and DDBO4Si8O20.32H2O are heteronetwork clathrates with 1,1,4,4-tetramethylpiperazinium (TMPA) and 1,4-dimethyl-1,4-diazoniabicyclo2.2.2octane (DDBO) guest cations. *Z. Anorg. Allg. Chem.* **1994**, *620*, 757–765. [CrossRef]
35. Wiebcke, M.; Koller, H. Single crystal X-ray diffraction and variable temperature MAS NMR study on the heterogeneous network clathrate Na(N(CH3)4)7Si8O20.54H2O. *Acta Crystallogr. Sect. B-Struct. Commun.* **1992**, *48*, 449–458. [CrossRef]